Heliyon 10 (2024) e27794

Contents lists available at ScienceDirect

Heliyon

journal homepage: www.cell.com/heliyon

Research article

Research on the destroy characteristics of PTFE/Cu composite liner to explosive reactive armor

Jianya Yi [a,*], Ruijie Hao [a], Xuezhi Tang [b], Siman Guan [a], Zhijun Wang [a], Jianping Yin [a]

[a] School of Mechatronic Engineering, North University of China, Taiyuan, 030051, PR China
[b] Chongqing Hongyu Precision Industry Group Co.Ltd, Chongqing, 402760, PR China

ARTICLE INFO

Keywords:
PTFE/Cu composites
Preparation process
Explosive reactive armor
Damage characteristics

ABSTRACT

The jet generated through PTFE based inert material liner has the characteristics of low energy, low density, and large aspect ratio, which can effectively achieve the "penetration without explosion" of explosive reactive armor. PTFE/Cu composite material liner with various densities is prepared, to research the roles of preparation procedure and density in the destroy effect of jet on reactive armor. Through numerical simulation research, it was found that there was no reaction at all in the explosive layer penetrated by the jet generated by the sinter liner molded, while the explosive layer penetrated by the jet generated through the hot-pressing sintering and extrusion molding liner experienced local reactions on the jet impact channel, and the overall explosive layer did not undergo any reaction. Through experimental verification, it has been proven that all three types of jets have achieved "penetration without explosion" on explosive reactive armor.

1. Introduction

In 1970, Held M proposed [1] to attach explosives to the outside of armored vehicles, so that they can use their own explosion to weaken the power of incoming ammunition, so as to achieve effective protection of armored vehicles. In 1974, Israel's Rafael Ordnance Bureau successfully developed explosive reactive armor and proposed the concept of driove-plate. According to previous experimental experience, the effect of the power of the single-layer reactive armor structure on the penetration effect of the traditional armor-piercing warhead is 70%–90% [2,3]. The damage to the explosive reactive armor (ERA) is mainly achieved by the front phase of the tandem warhead to "penetrate with explosion" the reactive armor, and then the target is damaged by the delayed rear warhead [4,5]. Held M analyzed the mutual effect between jet and reactive armor under different conditions and the launching process of reactive armor with shaped charge jet [6,7]. Gruau [8] studied the ignition criterion of plastic bonded explosive (PBX) under the framework of low velocity impact. Feng Zhu et al. [9] studied the response process of square metal sandwich plate with honeycomb core under explosion load. Youcai Xiao et al. [10] analyzed the destroy mechanism and related fracture mode of PBX under various impact loads, and established a PBX destroy constitutive model with viscoelastic reaction and statistical fracture. J.P. Curtis [11] analyzed the impact behavior of unconstrained explosives subjected to high-speed projectiles. Rosenberg Z [12] studied the interaction between normal incidence jet and reactive armor.

The above research analyzed the initiation mechanism of the jet to the explosive reactive armor at the theoretical level. There is

* Corresponding author.
E-mail address: yjy2020@nuc.edu.cn (J. Yi).

https://doi.org/10.1016/j.heliyon.2024.e27794
Received 17 July 2023; Received in revised form 29 February 2024; Accepted 6 March 2024
Available online 16 March 2024

Table 1
Ratio and preparation technology of PTFE/Cu material.

No.	PTFE/wt%	Cu/wt%	Theoretical density	Preparation technology
PTFE/Cu-1	63	37	3	Hot-pressing sintering
PTFE/Cu-2	49.5	50.5	3.5	
PTFE/Cu-3	40	60	4	
PTFE/Cu-4	63	37	3	Molded sintering
PTFE/Cu-5	49.5	50.5	3.5	
PTFE/Cu-6	40	60	4	
PTFE/Cu-7	63	37	3	Extrusion molding
PTFE/Cu-8	49.5	50.5	3.5	

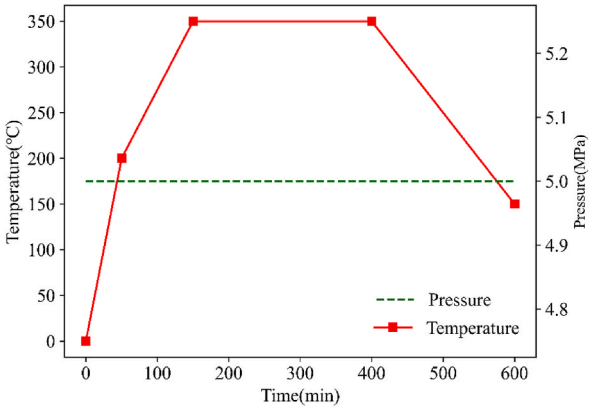

Fig. 1. Parameter setting of hot-pressing sintering process.

also a method to damage the subsequent targets without detonating the ERA. At present, ERA is mainly realized by shaped charge jet or explosively formed projectile. P. J. König [13] studied a pre-charged shaped charge, and derived the main characteristics of particle and solid jet penetration into ERA. Based on previous studies, when the reactive armor is penetrated by the jet without explosion, the liners are made of low-density inert materials or polymers, including polytetrafluoroethylene [14], glass [15], ceramics [16], etc. In addition to the above mentioned, there are also modified PTFE to modify the low-density PTFE, improve the material's jet energy and density, optimize the material's static and dynamic mechanical character. Through putting various fillers to PTFE matrix, the mechanical character of the material can be improved effectively, making it show better physical character than a single material [17,18]. Currently, the majority of studies of metal/non-metal propellant covers concentrate on active energetic materials based on PTFE or PTFE/AI. With the increasing popularity of reactive materials, a set of research on the formula [19], mechanical character [20], and damage mechanism [21] of PTFE matrix, has been made by a lot of scholars.

The jet generated through PTFE composite material performs better than conventional metal jet in certain fields. The jet displays a bigger aperture and shorter depth of penetration when penetrating thick steel plates [22]. With a greater penetration result, it is adopted as the liner material gradually [23]. The process of low-density jet was stimulated by Chang B H [24] with AUTODYN-2D finite element software. According to the outcomes, the mechanical character of polytetrafluoroe-thylene/copper (PTFE/Cu) are greatly enhanced compared with PTFE, and the jet shows great penetration ability. Under the equal structural circumstances, the PTFE/Cu jet to the face plate shows the penetration diameter increased by about 70%, and the back plate displays the penetration diameter increased by about 30%. However, in the above research, the preparation process of modified polytetrafluoroethylene is relatively simple.

Based on this, the impact initiation reaction armor tests of PTFE/Cu liners processed by various preparation procedures were made in this paper. The roles of various preparation procedures and densities of liners on the experiment results were compared and analyzed, and the impact response of ERA to jets with various preparation procedures and densities was obtained, which laid a theoretical foundation for the "penetration without explosion" damage technology of ERA.

2. Preparation of shaped charge liner

In this paper, PTFE with an average particle size of 220 μm and an average density of 2.2 g/cm^3 was selected. There was no real melting point. When heated to 327 ± 5 °C, it showed a non-flowing viscous melting state and no mechanical strength. When heated to 390 °C some PTFE began to decompose and produce tetrafluoroethylene toxic gas. Therefore, the heating temperature should not exceed 380 °C during sintering. For the research on the impact of various preparation procedures on the forming of PTFE/Cu materials were designed. Under each preparation process, a variety of composition ratios were designed, a total of 8 groups. The detailed composition ratio and preparation process are shown in Table 1.

Fig. 2. Hot-pressing sintering liner.

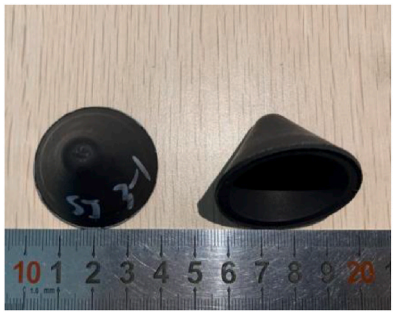

Fig. 3. Molded sintering liner.

2.1. Hot-pressing sintering

As a sintering approach, Hot-pressing sintering fills dry powder into a model, and then is heated in a uniaxial direction while pressing, to complete both molding and sintering simultaneously.

Because of the synchronous usage of temperature and pressure, diffusion, the contact, and flow features of particles are enhanced, resulting in easy plastic flow and densification and the thermoplastic powder with low deformation resistance. After a short time of heating and sintering, a composite material with uniform structure and certain densification can be obtained, that is, complete densification can be achieved by thermal consolidation. During the process, the pressure is applied and the temperature is raised at the same time. The pressure is constant, and the pressure is unloaded at the end of the temperature process to better eliminate the thermal stress inside the sample.

In this paper, given that the heat transfer effect of PTFE is poor, 327 °C is the crystallization transformation point With high melt viscosity, it is hard to flow; therefore, its sintering temperature shall be above 327 °C. In the meantime, with the purpose of improving the quality of the specimens acquired, the heating rate during sintering shall be concerned. Too fast heating rate will cause uneven expansion of PTFE in the mixed powder and cause cracking during specimen forming. The whole process of hot-pressing sintering was completed in argon atmosphere. The parameters of PTFE/Cu hot-pressing sintering process are set as shown in Fig. 1. Maintain the applied pressure at 5 MPa. Fig. 2 displays the shaped charge liner created through hot-pressing sintering.

2.2. Molded sintering

Its creation procedure should first pre-press the product in a certain shape of the mold, and then further heat the material to enhance the association between the powder particles for the necessary mechanical character.

The determination of the sintering temperature determines the crystallinity of the crystal in the composite material, thus affecting the final quality of the material. Based on this, the choice of the sintering temperature value is generally slightly greater than the melting point of PTFE, which can ensure that the PTFE crystal can be heated and then recrystallized. In this paper, according to the melting point of PTFE, it is decided that the sintering temperature is 380 °C. The molding pressure of PTFE/Cu samples with densities of 3 g/cm^3 and 3.5 g/cm^3 is 100 MPa, while the samples with densities of 4 g/cm^3 is 120 MPa. Fig. 3 shows the PTFE/Cu liner.

2.3. Extrusion molding

The approach means a creation approach for plastic materials to generate results from a hole mold under strong external forces. In the preparation process, the major elements influencing the properties of the modified polymer materials are the matching of the thread, the configuration speed of the screw, the extrusion temperature and pressure. Different extrusion temperatures also affect the

Fig. 4. Extrusion molding liner.

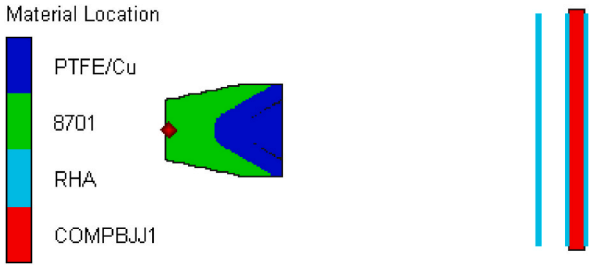

Fig. 5. Equivalent finite element model of explosive reactive armor.

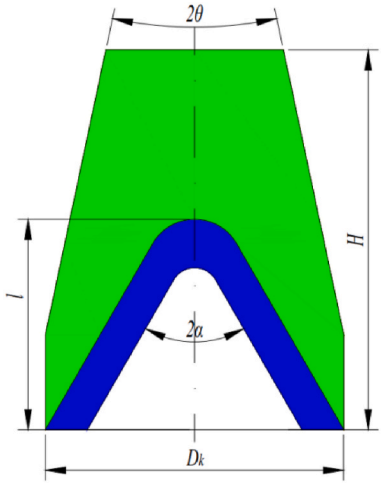

Fig. 6. Explosive structure diagram.

mechanical character of the material.Generally, the mechanical properties of the modified material increase first as temperature increases. If the temperature reaches a suitable value, the mechanical properties reach the optimum, and then the performance plummets. The suitable temperature generally refers to the glass transition temperature of polymers. For this paper, the suitable temperature value for polytetrafluoroethylene based composite materials is around 130 °C. In this paper, considering the significant differences in character between PTFE and Cu, a twin-screw extruder was adopted to directly process PTFE/Cu rods with various densities, and the rods were adopted to produce the required PTFE/Cu specimens and liners for the test, according to Fig. 4. During the extrusion process, the temperature was controlled at 360–400 °C and the pressure was 0.7 MPa.

3. Numerical simulation of PTFE/Cu jet penetrating explosive reactive armor

For the analysis of the damage features of explosive reactive armor by PTFE/Cu jet with various creation procedures, the numerical simulations were conducted using ANSYS/AUTODYN 19.2 for different PTFE/Cu liners. The numerical simulation of explosives and

Table 2
Shock equation of state coefficients and Johnson-Cook coefficients of PTFE/Cu material.

Liner No.	Preparation procedure	ρ (g/cm^3)	Gruneisen parameter	C_1	S_1	Yield strength (MPa)	Hardening constant (MPa)
1#	Hot-pressing sintering	3	2.7482	2.1433	1.7045	17.13	32.726
2#		3.5	2.7915	1.9671	2.2286	20.31	34.507
3#		4	2.8073	2.0327	1.7881	19.47	46.680
4#	Molded sintering	3	2.7482	2.1662	1.7472	12.16	40.083
5#		3.5	2.7915	2.1218	1.7064	16.72	48.122
6#		4	2.8073	2.0732	1.8137	20.396	60.039
7#	Extrusion molding	3	2.7482	2.1175	1.7329	14.35	16.306
8#		3.5	2.7915	2.1792	1.1618	9.73	41.897

Table 3
JWL equation of state coefficients and C-J coefficients of 8701 explosive.

A (GPa)	B (GPa)	R_1	R_2	W	ρ (g/cm^3)	D (m/s)	E (KJ/m^3)	P_{CJ} (GPa)
854.5	20.493	4.6	1.35	0.25	1.71	8315	8.5e6	29.5

Table 4
Material coefficients of RHA.

ρ (g/cm^3)	$\gamma(V)$	C_0(m/s)	S	Shear modulus (Gpa)	Yield strength (Gpa)
7.86	1.67	4610	1.73	64.1	1.5

shaped charge liners adopt the SPH algorithm with a particle gap of 0.05 cm. The steel target of explosive reaction armor adopts the Lagrange algorithm with a mesh size of 0.1 cm.

In this paper, the numerical emulation of the explosive reactive armor "PBFY-1" is carried out. The explosive reactive armor is composed of shield plate, rib, face plate, explosive layer and back plate. The shield plate and face plate are connected by two ribs in the middle. The face plate and the back plate are connected by screws, and the explosive is sealed. The shield plate shows the thickness of 3 mm, and the face plate and the back plate are 2 mm thick; the explosive layer is 4 mm thick.

In the calculation of numerical modelling, the explosive reactive armor of PBFY-1 is equivalent to a certain extent. Fig. 5 shows the equivalent finite element model. The formed charge warhead conforms to the penetration simulation model. The materials of shield plate, face plate and back plate are Rolled Homogeneous Armor (RHA), and the intermediate layer charge is COMPBJJ1 explosive.

The structural diagram is shown in Fig. 6. With the stern width of 22 mm and the angle of $2\theta = 24^\circ$, and the liner shows the same thickness as the arc cone integrated liner. The cone top shows the radius of 6 mm, the wall thickness of $\delta = 3$ mm, and the liner displays the cone angle of $2\alpha = 60^\circ$; the liner is $l = 26.04$ mm high, and the charge shows the diameter of $D_k = 37$ mm; the charge shows the height of $H = 47$ mm.

Johnson-Cook is the constitution model of PTFE/Cu material. The Shock equation of state is shown in Eq. (1):

$$U_s = C + SU_p \tag{1}$$

Among them, C is the material sound velocity, and S is the material constant.

The expression for the *Grüneisen* coefficient is shown in Eq. (2) [25].

$$\gamma(V) = \frac{B}{6\delta^{1/3}} \cdot \frac{4\ exp\left[2B\left(1-\delta^{-1/3}\right)\right] - exp\left[B\left(1-\delta^{-1/3}\right)\right]}{2\ exp[2B(1-\delta^{-1/3})] - exp[B(1-\delta^{-1/3})]} \tag{2}$$

Among them, A and B are the parameters measured in the experiment; $\delta = \frac{V_{0K}}{V}$ is compressibility at zero temperature.

Table 2 shows the specific coefficients.

Explosive 8701 is chosen as the explosive, and the detonation procedure of explosive is described with JWL state equation. Eq. (3) [25] shows the JWL equation of state:

$$p = A\left(1 - \frac{\omega}{R_1 V}\right)e^{-R_1 V} + B\left(1 - \frac{\omega}{R_2 V}\right)e^{-R_2 V} + \frac{\omega E_0}{V} \tag{3}$$

Among them, p is the pressure; A, B, R_1, R_2, ω mean constants; E_0 stands for the internal energy per unit volume of explosive. Table 3 shows the specific coefficients.

Among them, ρ means the mean density of the major charge formed for the test, D stands for the velocity of detonation, E refers to the density of energy per unit volume, and P_{CJ} stands for the explosive's detonation pressure.

RHA material uses Shock state equation commonly used in high-speed impact numerical simulation. The strength model is Von Mises model, and the failure model is Plastic Strain model. Table 4 shows the specific material parameters.

Table 5
Lee-Tarver model coefficients of COMPBJJ1 explosive.

ρ (g/cm^3)	JWL	A(Gpa)	B(Gpa)	R_1	R_2	W	D(m/s)
1.717	Detonation products	524.2	7.678	4.2	1.1	0.34	7980
	Unreacted	77810	−5.031	11.3	1.13	0.8938	–
P_{CJ}(Gpa)	I(μs^{-1})	b	a	x	G_1	c	d
29.5	44	0.222	0.01	4	414	0.222	0.667
Y	G_2	E	G	Z	F_{igmax}	F_{G1max}	F_{G2min}
2	0.0	0.0	0.0	0.0	0.3	1	1

Table 6
Parameters of experiment.

Reaction armor No.	Liner type	Density (g/cm^3)	Penetration angle (°)	Stand-off
1#	Hot-pressing sintering	3.5	90	3D
2#		4	90	3D
3#	Molded sintering	3.5	90	3D
4#		4	90	3D
5#	Extrusion molding	3.5	90	3D

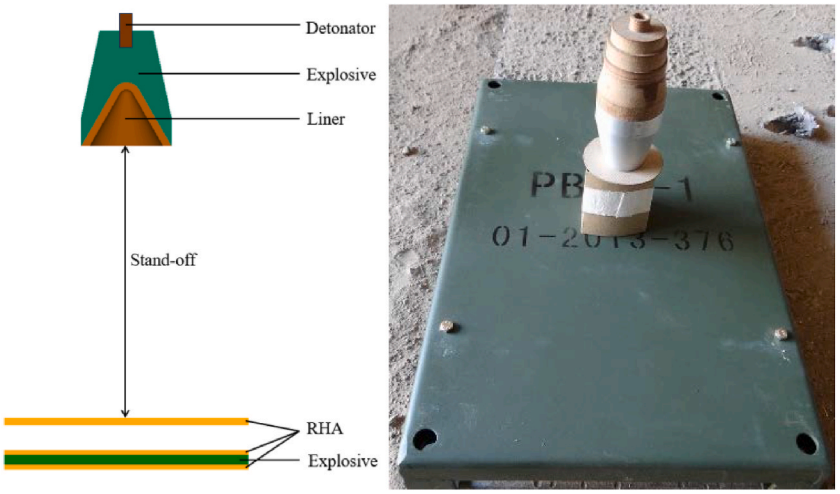

Fig. 7. Experimental setting of explosive reactive armor.

Complete detonation and shock initiation of explosives require different state equations to describe the performance of explosives. The state of the impact can be described by the Lee-Tarver model in the numerical simulation process. The model divides the impact state of heterogeneous explosives into the phases of ignition, increase and ending, and considers that ignition starts from local hot spots and then propagates to the surrounding through these local hot spots. Eq. (4) [25] shows the reaction rate equation of the Lee Tarver model:

$$\frac{\partial F}{\partial t} = I(1-F)^b(\mu-\alpha)^X + G_1(1-F)^e F^d P^y + G_2(1-F)^e F^g P^z \tag{4}$$

In the formula, F is the explosive reaction ratio (the proportion of the mass of the exploded explosive to the total mass of the explosive), and t is the time, μ is the compressibility, P means the pressure in the explosive, and I, G_1, G_2, a, b, x, c, d, y, e, g and z stand for explosive related parameters. This model includes two JWL equations and a trinomial reaction rate equation. The reactants are described with the first JWL equation of state, and the detonation results are described. Table 5 shows the Lee-Tarver model coefficients of COMPBJJ1 explosive.

4. Experimental verification of penetrating explosive reactive armor

A total of 5 sets of PTFE/Cu jet impact reactive armor were carried out. Table 6 shows the liner and experiment coefficients. The schematic diagram of the jet impact reactive armor is shown in Fig. 7, in which the liner is stern type, the density is 1.71 g/cm^3,

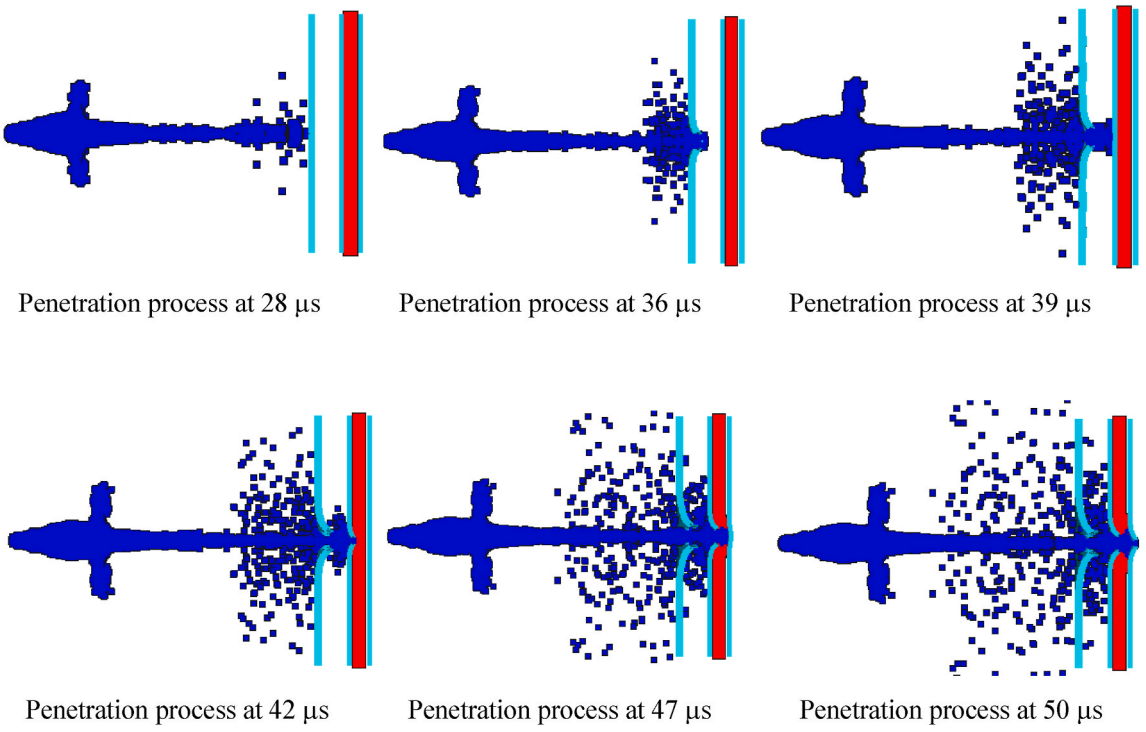

Fig. 8. The penetration process of ERA by jet.

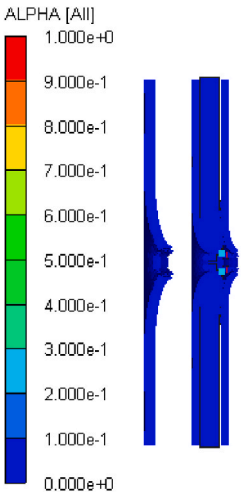

Fig. 9. Explosive reactivity nephogram (3.5 g/cm^3, hot-pressing sintering).

the stand-off is 3 times the charge diameter, and the sandwich explosive is insensitive explosive.

During the experiment, the explosive was detonated by the detonator, and the high-temperature and high-pressure gas formed by the detonation of the explosive overwhelmed the liner. The jet gradually stretched at the stand-off, and after the jet head speed reached a certain value, it started penetrating the explosive reactive armor.

5. Results and discussion

5.1. The role of the preparation procedure of the liner in the impact to ERA

5.1.1. Numerical simulation results

Fig. 8 is the process of jet penetrating explosive reactive armor. At 28 μs, the jet reaches the shield plate of the reactive armor. In the

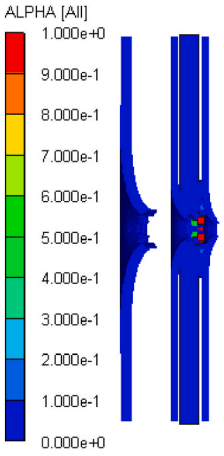

Fig. 10. Explosive reactivity nephogram (3.5g/cm^3, molded sintering).

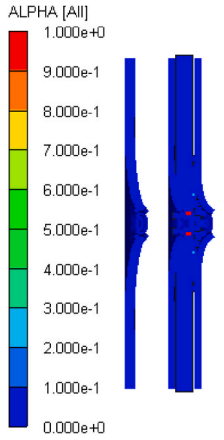

Fig. 11. Explosive reactivity nephogram (3.5 g/cm^3, extrusion molding).

meantime, the material of the jet head is hindered by the shield plate. Some of the forward movement begins to penetrate the shield plate, and the other part begins to fly around the shield plate. The jet completely penetrates the shield plate at 36 μs. At 39 μs, the jet began to act on the face plate and formed a precursor shock wave in the face plate. At this time, the jet head velocity was 4358 m/s. At 42 μs, while completely penetrating the face plate, the jet squeezes the explosive to deform. At this time, the jet head shows the residual velocity of approximately 1890 m/s. At 47 μs, the jet passes through the explosive and begins to penetrate the back plate. The residual velocity of the jet head is around 1573 m/s. At 50 μs, the jet completely passes through the reactive armor, and the jet head shows the residual velocity of approximately 1386 m/s. The jet shows greatly attenuated head velocity when penetrating the shield plate and the face plate, while the explosive does not exerts a great effect on the head velocity. Fig. 9 shows that the explosive layer of ERA basically did not react, indicating that the PTFE/Cu processed by hot-pressing sintering achieved “penetration without explosion” of ERA. From the morphology of the penetration channel left on the explosive reactive armor after the penetration, the jet on the shield plate shwos the penetration diameter of approximately 20 mm, and the face plate displays thepenetration diameter of about 12 mm; the back plate shows the penetration diameter of about 30 mm.

Fig. 10 shows the explosive reactivity nephogram after the jet generated through the molded sintering liner penetrates the ERA. The explosive layer in the ERA experienced local reactions on the jet penetration channel, but the overall explosive layer did not explode, indicating that the molded sintering PTFE/Cu jet realized the “penetration without explosion” of the ERA. From the morphology of the penetration channel left on the explosive reactive armor after the penetration, the jet on the shield plate shows the penetration diameter of about 19 mm, and the face plate displays the penetration diameter of about 13 mm; the back plate shows the penetration diameter of about 26 mm.

Fig. 11 is the explosive reactivity nephogram after the jet generated through the extrusion forming liner penetrates the ERA. The explosive layer reacts locally on the jet penetration channel, but the overall explosive does not react, indicating that the extrusion molding PTFE/Cu jet realizes the “penetration without detonation” of the explosive reactive armor. From the morphology of the penetration channel left on the ERA after the penetration, the jet into the shielding plate shows the penetration diameter of about 24

Table 7
The penetration diameter of the jet generated by various process liners to the ERA plates (mm).

Target plate	Hot-pressing sintering	Molded sintering	Extrusion sintering
Shield plate	20	19	24
Face plate	12	13	13
Back plate	30	26	24

(a) Experiment result diagram

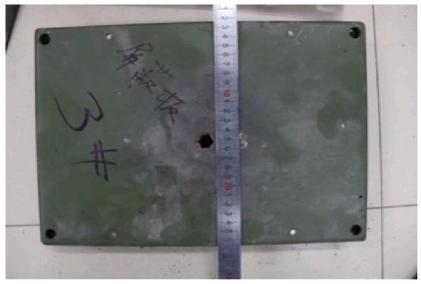

(b) Damage effect diagram of shield plate

(c) Damage effect diagram of face plate

(d) Damage effect diagram of back plate

Fig. 12. Experimental results of 1#ERA.

mm, and the panel displays the penetration diameter of 13 mm; the back plate displays the penetration diameter of about 24 mm.

The jets formed by the shaped charge liners under three different preparation processes all achieve the "penetration without explosion" of the ERA, but the explosive layer generated by the jet penetration does not react at all, while the jet penetration have local reaction on the jet impact channel, but the overall explosive layer does not react.

From Table 7, the jet generated by the liner prepared by extrusion molding has the largest penetration diameter to the shield plate and the smallest of molded sintering. The jet has the largest penetration diameter to the back plate, while the jet has the smallest penetration diameter to the back plate. The penetration diameters of the three jets on the face plate are not much different.

(a) Experiment result diagram

(b) Damage effect diagram of shield plate

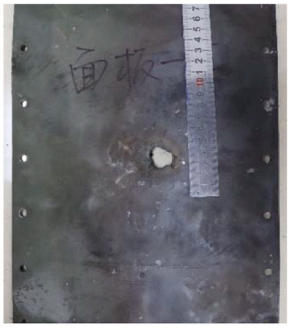

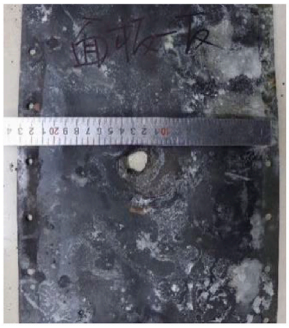

(c) Damage effect diagram of face plate

(d) Damage effect diagram of back plate

Fig. 13. Experimental results of 3#ERA.

5.1.2. Experiment verification results

Fig. 12 shows the experimental results of jet impact reactive armor generated by hot-pressing sintering PTFE/Cu liner. The figure shows that the ERA is not detonated, that is, the jet realizes the penetration of the reactive armor without explosion. Fig. 12(a) displays that the sandwich charge does not undergo detonation reaction.The face plate of the reactive armor appears a circular reaction zone of suspected sandwich charge, which is close to the size of the hole on the back plate. In addition, the rest of the charge is complete and no reaction occurs, which is the same as the simulation results. Fig. 12(b) displays that the jet penetrating the shield plate shows the complete hole, and the diameter is about 19.00 mm.

By analyzing Fig. 12(c) and (d), the shape of the hole on the face plate of the reactive armor is consistent with that of the shield plate, showing a concave round hole. The concave direction is consistent with the direction of the incident jet. The back plate has a large hole, which is an irregular eversion petal type, and the eversion direction conforms to the direction of the jet hole.

From the experimental results of Fig. 13, in case of the molded sintering liner with the density 3.5 g/cm^3, the jet can realize "penetrate without explosion" to the ERA, but the sandwich charge is partially burned, mainly concentrated near the jet penetration channel, as shown in Fig. 13(a) (c). The penetration hole of the shield plate is circular, with an aperture of 17.00 mm. There is Cu in the jet around the hole. As shown in Fig. 13(b) (d), the hole of the panel is circular, and the hole of the back plate is irregular, showing a tearing and eversion shape.

The jet generated through the PTFE/Cu liner processed by extrusion molding was subjected to an impact initiation reaction armor experiment. The results are shown in Fig. 14.

Fig. 14(a) shows that the extrusion molding liner also achieves "penetration without explosion" to the reactive armor. Obviously,

(a) Experiment result diagram

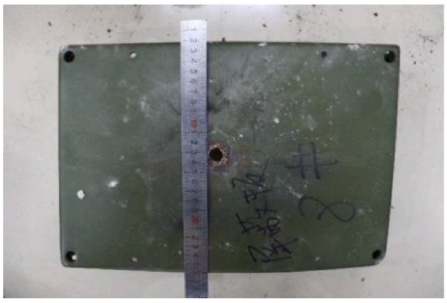

(b) Damage effect diagram of shield plate

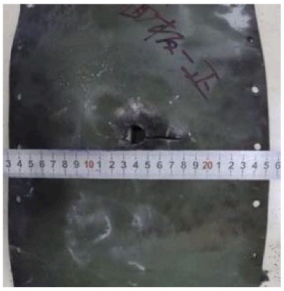

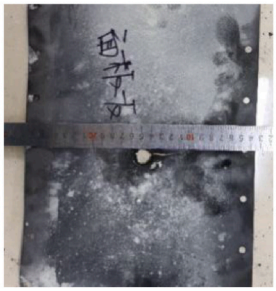

(c) Damage effect diagram of face plate

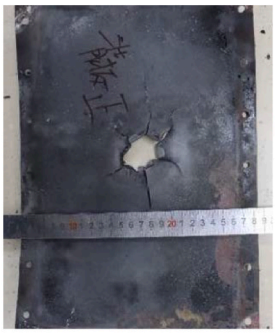

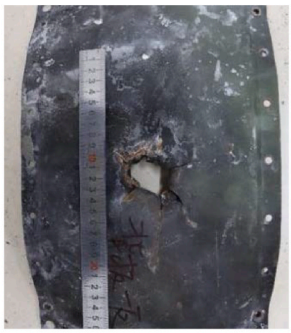

(d) Damage effect diagram of back plate

Fig. 14. Experimental results of 5#ERA.

Table 8
Comparison of penetration aperture of jet to shield plate under numerical simulation and experimental verification.

	Hot-pressing Sintering	Molded Sintering	Extrusion molding
Numerical Simulation	20	19	24
Experiment Verification	19	17	24

the face plate and back plate of the reactive armor have obvious burning black smoke, indicating that the local combustion reaction of the reactive armor sandwich charge occurs. Fig. 14(b) displays that the hole generated through penetrating the jet into the shield plate is circular, with an aperture of 24 mm, and a thick layer of red material is attached to the periphery of the hole, which should be the residual material of the jet with Cu as the main body. From Fig. 14(c), the holes formed by the extrusion molding liner face plate are concave circles, which are consistent with the direction of the jet inflow. From Fig. 14(d) diagram, it can be seen that although the back plate is obviously arched outward, the damage direction of the holes is opposite to the direction of the jet impact, which is concave, the shape is like petal shape, and the radial penetration cracks of the holes are obvious. It shows that although the jet generated through the extrusion molding liner can “penetration without explosion” the reactive armor, the hole features shaped by the jet differ from those of other preparation methods.

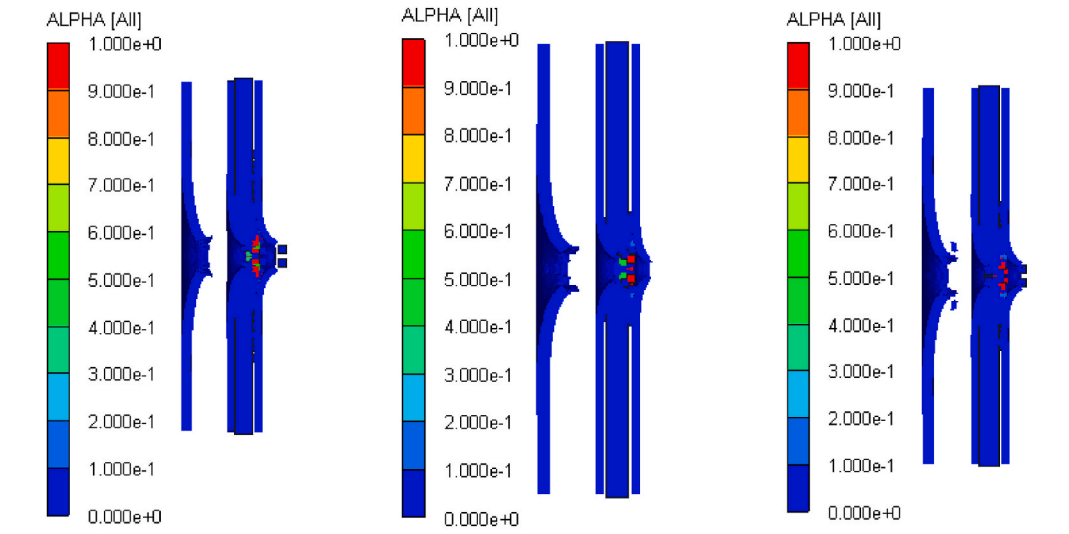

Fig. 15. The nephogram of explosive layer after jet impact formed by different density liners.

Table 9
Penetration diameter of the jet generated by various density liners to the ERA plate (mm).

Target plate	3 g/cm^3	3.5 g/cm^3	4 g/cm^3
Shield plate	20	19	18
Face plate	13	13	12
Back plate	28	26	20

Table 8 is the comparison of the penetration diameter results of jets with various preparation procedures on the shield plate under the conditions of modeling and experimental validation. The table shows not much varied results of numerical modeling and experimental validation, which can illustrate the accuracy of numerical simulation.

5.2. The role of the density of the liner in the impact to ERA

5.2.1. Numerical simulation results

The effect of density was analyzed by numerical simulation of the jet impact reaction armor formed by the molded sintering liner at three densities.

Fig. 15 shows that the explosive layer generated through the jet impact of the three density liners has a local reaction on the jet channel, but the explosive layer does not react as a whole. It can be considered that the jets of the three densities have realized the "penetration without explosion" of the ERA.

Table 9 is the penetration diameter of the jet generated by various density liners to the reactive armor plate. As density grows, the jet to the shield plate, face plate and back plate of the reactive armor shows gradually declining penetration diameter. This is because as density increases, the characteristics of the jet are close to the metal Cu jet, and the hole expansion performance is weakened.

5.2.2. Experiment verification results

The comparative experiments of impact initiation of reactive armor were carried out by using the molded sintering PTFE/Cu liners. The experiment results are shown in the following figures.

From the experimental results of Fig. 16 and Fig. 17, in case of the liner density of 3.5 g/cm^3 and 4 g/cm^3, the jet realizes "penetration without explosion" to the reactive armor, but the damage form and degree of the face plate and back plate of the ERA are different. Among them, the reactive armor sandwich charge of the 3# ERA is partially burned, mainly concentrated near the jet penetration channel, as shown in Fig. 16(a). While the reactive armor sandwich charge of the 4#ERA is burned, the charge shell has obvious deformation, and the back plate has obvious jet residual material, according to Fig. 17(a). Despite varied density, the penetration holes of the two kinds of jets on the reactive armor are circular, and the apertures are 17.00 mm and 20.00 mm respectively. Among them, there are a few red substances around the holes of the shield plate in the 3#ERA, which should be Cu in the

(a) Experiment result diagram

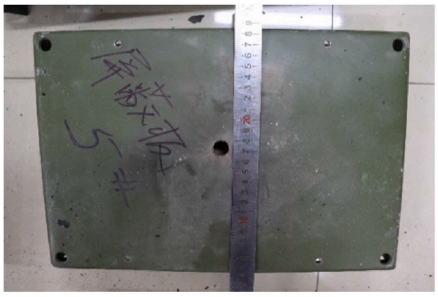

(b) Damage effect diagram of shield plate

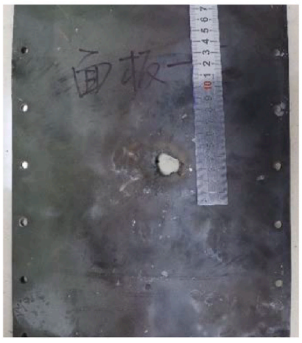

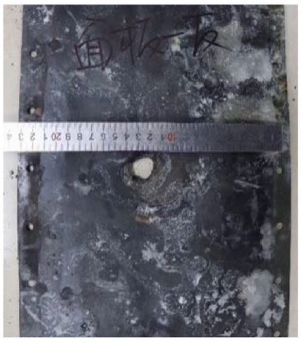

(c) Damage effect diagram of face plate

(d) Damage effect diagram of back plate

Fig. 16. Experimental results of 3#ERA.

jet, according to Fig. 16(b) (c) (d). Fig. 17(c) and (d) show that there is no obvious jet residue on the face plate and the back plate. The jet penetration holes of the face plate are circular, the back plate holes are irregular, and the whole is petal-shaped. Obviously, the sandwich armor near the holes reacts, but it does not reach the detonation reactivity of the explosive. Different from the impact degree of 3#ERA, the shield plate of 4#ERA has obvious jet residual material around the penetration hole, which is splashed around the hole, accordign to Fig. 17(b). Fig. 17(c) and (d) display different penetration holes of the face plate and the back plate of the reactive armor. The holes of the face plate are circular, and the holes of the back plate are irregular, which are similar to the shape of the superposition of two circles. Some of them are consistent with the shape of the face plate holes, and the other part is torn and eversion.

6. Conclusion

The damage features of ERA by PTFE/Cu jets with various preparation procedures and densities are researched herein, which lays a theoretical foundation for the “penetration without explosion” damage technology of explosive reactive armor. The major conclusions of this paper are shown below.

(1) Through numerical simulation, the jets generated through the liners under three different preparation procedures all achieve the “penetration without explosion” of the explosive reactive armor, but the jet penetrating explosive layer generated by the

(a) Experiment result diagram

(b) Damage effect diagram of shield plate

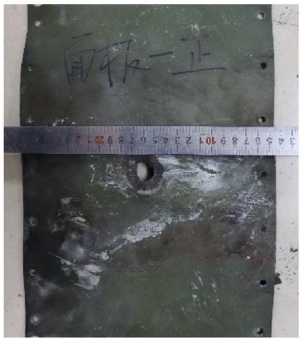

(c) Damage effect diagram of face plate

(d) Damage effect diagram of back plate

Fig. 17. Experimental results of 4#ERA.

hot-pressing sintering liner does not react at all, while the jet penetrating explosive layer generated by the molded sintering and extrusion liner has a local reaction on the jet impact channel, and the overall explosive layer does not react.

(2) The jet generated through the shaped charge liner created through extrusion molding has the largest penetration diameter to the shield plate and the smallest molded sintering liner. The jet has the largest penetration diameter to the back plate, while the jet has the smallest penetration diameter to the back plate. The penetration diameters of the three jets on the face plate are not much different.

(3) As density increases, the characteristics of PTFE/Cu jet is close to the Cu jet gradually, so the penetration diameter of the shield plate, face plate and back plate of the ERA gradually decreases.

(4) It is verified by experiments that the jets formed by the liners prepared by the three processes all realize the “penetration with explosion” of the ERA. This can provide theoretical support for the penetration without explosion damage technology of shaped charge jet to explosive reactive armor.

CRediT authorship contribution statement

Jianya Yi: Writing – original draft, Validation, Methodology. **Ruijie Hao:** Software, Investigation. **XueZhi Tang:** Data curation. **Siman Guan:** Software, Investigation. **Zhijun Wang:** Writing – review & editing, Methodology. **Jianping Yin:** Writing – review & editing.

Declaration of competing interest

The authors declare that they have no known competing financial interests or personal relationships that could have appeared to influence the work reported in this paper.

References

[1] M. Held, Stopping power of explosive reactive Armours against different shaped charge diameters or at different angles[J, Propellants, Explos. Pyrotech. 26 (2001) 97–104.
[2] X.Q. Ma, F.J. Zeng, M.L. Chen, et al., A new approach in anti-reactive armor, Acta Armamentarii 15 (4) (1994) 75–79.
[3] T.H. Bootes, M. Castillo, Missile Warhead design[P], US Patent, 1999 5939662.
[4] S. Harikrishnan, K. Murthy, Inconsistent performance of a tandem-shaped charge warhead, Defence Sci. J. 60 (2) (2010).
[5] K. Naeem, A. Hussain, et al., A comparative numerical and experimental study of light weight materials for neutralizing explosive reactive armour, Cent. Eur. J. Energ. Mater. 18 (2) (2021) 271–286.
[6] M. Held, Analysis of the shaped charge jet induced reaction of high explosives, Propellants, Explos. Pyrotech. 14 (6) (1989).
[7] M. Held, Discussion of the Experimental Findings from the initiation of covered, but unconfined high explosive charges with shaped charge jets[J, Propellants, Explos. Pyrotech. 12 (5) (1987).
[8] C. Gruau, D. Picart, R. Belmas, et al., Ignition of a confined high explosive under low velocity impact, Int. J. Impact Eng. 36 (4) (2008).
[9] F. Zhu, L. Zhao, G. Lu, et al., A numerical simulation of the blast impact of square metallic sandwich panels, Int. J. Impact Eng. 36 (5) (2008).
[10] Y. Xiao, Y. Sun, Y. Zhen, et al., Characterization, modeling and simulation of the impact damage for polymer bonded explosives, Int. J. Impact Eng. 103 (2017).
[11] J. Curtis, J. Mills, N. Lynch, et al., An analytical model for high velocity impact on confined explosive configurations, Int. J. Impact Eng. 33 (1) (2006).
[12] Z. Rosenberg, E. Dekel, On the interaction between shaped charge jets and confined explosives at normal incidence, Int. J. Impact Eng. 23 (1) (1999).
[13] P.J. König, F.J. Mostert, A parameter study of the non-initiating defeat of ERA by low density granular jets[C], in: Proceedings of 20th International Symposium on Ballistics, Orlando, 2002.
[14] J. Yi, Z. Wang, J. Yin, et al., Reaction characteristics of polymer expansive jet impact on explosive reactive armour, E-Polymers 20 (1) (2020).
[15] L.L. Ding, W.H. Tang, X.W. Ran, Simulation study on jet formability and damage characteristics of a low-density material liner, J. Mater. 11 (No.1) (2018) 72.
[16] M. Ly, S. Spinelli, S. Hays, et al., 3D printing of ceramic biomaterials, Engineered Regeneration 3 (No.1) (2022) 41–52.
[17] D.P. Gu, L.X. Zhang, S.W. Chen, K.F. Song, S.Y. Liu, Optimization of PTFE/Cu/Al_2O_3 filled PMMA based composites on tribologicalproperties using Taguchi design method, Appl Polym Sci 135 (45) (2018).
[18] J. Huang, X. Fang, Y. Li, et al., The mechanical and reaction behavior of PTFE/Al/Fe2O3 under impact and quasi-static compression, Adv. Mater. Sci. Eng. 2017 (2017).
[19] Xuezhi Tang, Zhijun Wang, Xuepeng Zhang, et al., Comparative study on microstructure and properties of different designed PTFE/Cu materials, J. Mater. Res. Technol. (17) (2022) 1512–1521.
[20] B. Feng, X. Fang, H. Wang, et al., The effect of crystallinity on compressive properties of Al-PTFE, Polymers 8 (10) (2016).
[21] H. David, Correlation between shaped charge jet break up and grain boundary impurity concetrations[C], The Proceedings of 13rd Int Symp on Ballistics. Stockholm. 549 (1992).
[22] H. Guo, Y. Zheng, Q. Yu, et al., Penetration behavior of reactive liner shaped charge jet impacting thick steel plates, Int. J. Impact Eng. 126 (2018).
[23] Pyrotechnics, Enhanced damage effects of multi-layered concrete target produced by reactive materials liner, Journal of Technology & Science (2018).
[24] B.H. Chang, J.P. Yin, Z.Q. Cui, T.X. Liu, Numerical simulation of modified low-density jet penetrating shell charge, Int. J. Simulat. Model. 14 (2015) 426–437.
[25] Century Dynamics, AUTODYN Explicit Software for Nonlinear Dynamics Theory Manual[Z], Century Dynamics Inc., U.S.A., 2005.